United Nations ECE/TRANS/WP.5/GE.3/2016/3/Rev.1

Economic and Social Council

Distr.: General
20 June 2017

Original: English

Economic Commission for Europe

Inland Transport Committee

Working Party on Transport Trends and Economics

Group of Experts on Climate Change Impacts and Adaptation for Transport Networks and Nodes

Thirteenth session
Geneva, 22 and 23 June 2017
Item 4 of the provisional agenda
Discussions on the final report of the Group of Experts

An Overview of Recent Climate Change Trends and projections affecting transportation in the ECE Region (Part I)

Note by the secretariat*

I. Mandate

1. This document has been prepared in line with the output/activities of cluster 2: "Transport trends and economics (including Euro-Asian transport links)" of the programme of work of the transport subprogramme for 2016-2017 (ECE/TRANS/2016/28/Add.1, para. 2.2) and the Terms of Reference of the United Nations Economic Commission for Europe (UNECE) Group of Experts on Climate Change impacts and adaptation for transport networks and nodes (ECE/TRANS/2015/6) as adopted by the Inland Transport Committee on 24-26 February 2015 (ECE/TRANS/248, para. 34).

II. Climate Change: Recent Trends and Projections

2. The information presented here focuses on climatic factors the variability and change of which can have significant implications on transport. Some of the information (climatic factor trends/projections until 2013) has been presented in a previous ECE report

* This document was submitted late due to delayed inputs from other sources.

GE.17-10190(E)
1710190

(ECE, 2013); in this (draft) report, focus is placed on the most recent 6-year period (2011-2016) as well as on the recent projections on Climate Variability and Change (CV & C)[1].

A. Climate Change Trends

3. There is overwhelming evidence for a warming world since the nineteenth century from independent scientific observations in different environments (from the upper atmosphere to the ocean deeps). Nevertheless, in most cases, discussions on Climate Change focus on the land surface temperature increase, which is only just one of the indicators of changing climate, with others being changes in e.g. the atmospheric/oceanic temperature, sea level, precipitation, and glacier, snow and sea ice covers (Fig. 1).

Figure 1

Change of climatic factors

(Each line represents an independently derived estimate. In each panel all data sets have been normalized to a common period of record (IPCC, 2013))

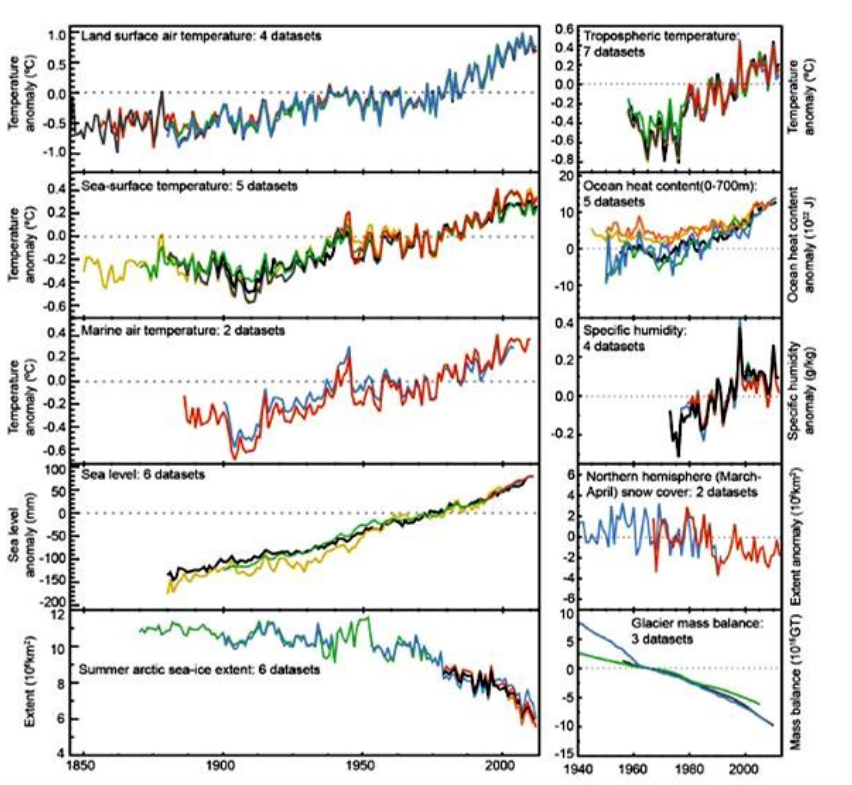

4. Temperature increases have been observed in the troposphere during the last decades. The oceans, which may have absorbed more than 80 per cent of the excess energy associated with the increased emissions since the 1970s, show significant increases in heat content (IPCC, 2013; Melillo et al., 2014; Dieng et al., 2017); these have resulted in steric increases of the sea level that are considered as a main driver of sea level rise-SLR (Hanna et al., 2013). At the same time, glacier and sea ice covers have been declining over the last

[1] Note that Climate Variability and Change (CV & C) refers to the variability and sustained change of climatic conditions relative to a reference period, e.g. the first period with accurate records (1850s-1860s) or periods at which infrastructure used today has been constructed (e.g. 1961-1990 or 1986-2005).

few decades. Arctic sea ice has decreased by > 40 per cent since satellite records began (1979), particularly at the end (in September) of the annual melt season (Melillo et al., 2014; NOAA, 2017a). Glacier ice has been consistently decreasing during the last 20 years and spring snow cover has also shrunk across the Northern Hemisphere-NH since the 1950s (IPCC, 2013; NSIDC, 2017).

1.1.1 Temperature and precipitation

5. Globally-averaged, near-surface temperature is the most cited climate change indicator as it is directly related to (i) the planetary energy balance (Fourier 1827) and the increase in cumulative Greenhouse Gas-GHG emissions (IPCC, 2013), and (ii) many climatic impacts and risks (Arnell et al., 2014). Although each year (or decade) is not always warmer than the previous, there has been a long-term warming trend (Fig. 2). Most of the warming occurred in the past 35 years (NASA, 2016).

Figure 2

Global average temperature anomalies for the period 1850-2016 relative to the reference period 1961-1990 for 3 major datasets[2]

(Grey shading indicates the uncertainty in the HadCRU dataset (UK Met Office Hadley Centre) (From WMO, 2017))

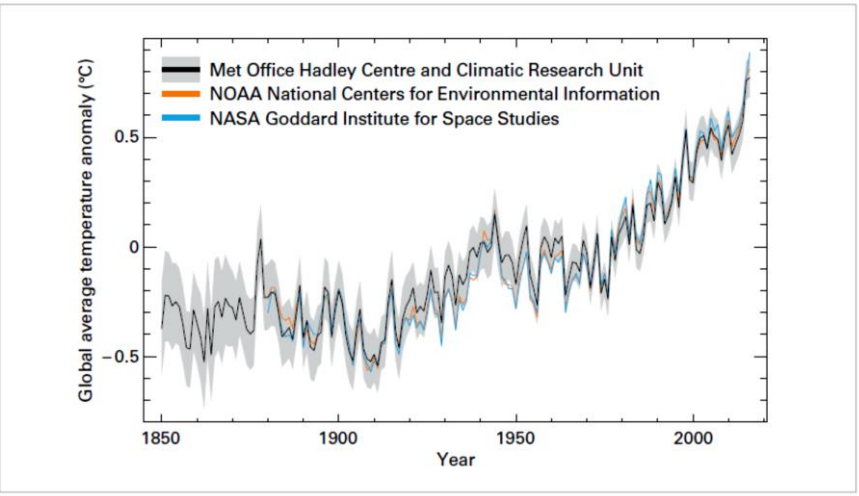

6. 2016 has been the warmest year in the instrumental record, breaking the previous records of 2015 and 2014, with the data being consistent with a steady global warming trend since the 1970s, superimposed on random, stationary, short-term variability (Rahmstorf et al., 2017). It is the third year in a row that global average surface temperature set a new record, and the fifth time the record has been broken since the start of the twenty-first century (NOAA. 2017b).

7. Warming of the climate system is unequivocal; all observations suggest increases in global average surface air and ocean temperatures (IPCC, 2007; 2013). The planet's average surface temperature has risen by 1.1 ^{0}C since the late nineteenth century, a change largely driven by increased atmospheric concentrations in GHGs. Globally averaged land and ocean surface temperature in 2015 was about 0.76 ± 0.09 ^{0}C above the 1961-1990

[2] In the WMO (2017) analysis, the latest versions of the 3 datasets: GISTEMP, NOAAGlobalTemp and HadCRUT maintained, by NOAA, the US National Air and Space Administration (NASA) and the UK Met Office Hadley Centre have been used. The combined dataset extends back to 1880 (WMO, 2017. http://library.wmo.int/opac/doc_num.php?explnum_id=3414).

average (94 per cent certainty, NASA (2016)), whereas the third in order world breaking record year was 2014 (MetOffice, 2014).

8. Since the beginning of the twenty-first century, there has been a slowdown in the rate of the global mean surface temperature rise compared to global climate model projections. Over the period 2003-2013, both global land and sea surface temperatures increased at a lower rate than in the previous decades (Dieng et al., 2017). This apparent slowdown (termed as '*the global warming hiatus'*) has been also attributed to uncertainties in the simulations of the conventional datasets related to external climate forcing, such as volcanic eruptions, stratospheric changes in water vapour and industrial aerosols, heat redistribution within the oceans, solar activity and the inter-annual to decadal variability of ocean cycles (e.g. El Niño and La Niña events) (IPCC, 2013; MetOffice, 2014; Fyfe et al., 2016; Yan et al., 2016). Recent research (e.g. Cowtan and Way, 2014; Karl et al, 2015; Simmons et al., 2017) has questioned the occurrence of *the global warming hiatus* in the rising temperature trend, suggesting that there were biases in surface temperature datasets and that re-analysis of corrected/updated data indicate that recent global temperature trends are higher than those reported in previous studies (e.g. IPCC, 2007; 2013).

Figure 3

Annual temperatures compared to 1951-1980 average

(Blue and red bars represent the annual temperature anomalies in El Niño and La Niña years, respectively. Blue and red lines are the trends; neutral years in grey; the dashed line represents the overall trend (NASA, 2016))

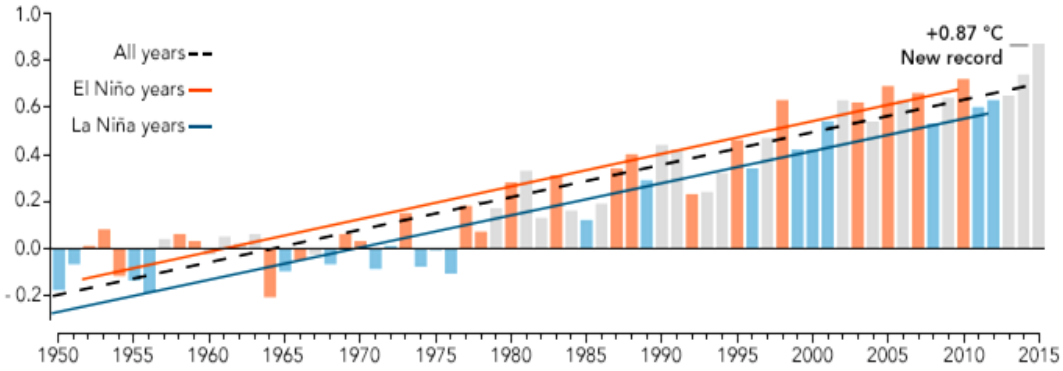

9. Generally, years starting during an El Niño event are warmer than non El Niño years i.e. neutral or La Niña years (Fig. 3). The 2015 and 2016 temperature records were influenced by the strong El Niño conditions in the Pacific (NASA, 2016). In 2014, however, near surface land temperatures were 0.88 ± 0.20 ^{0}C higher than the 1961-1990 average according to NOAA estimates (WMO, 2014), although it was a neutral El Niño year. In 2016, record temperatures were widespread at the Northern Hemisphere (NH), particularly in Arctic regions (Fig. 4). In early 2016, the global temperature was about 1.5 ^{0}C above that recorded in the early industrial revolution and > 0.4 ^{0}C higher than that recorded in 1998 (also a strong El Nino year) (Simmons et al., 2017).[3] Alaska experienced unprecedented, widespread warming (NSIDC, 2017). Globally averaged sea surface temperatures (SSTs) were also the warmest on record, with the anomalies being strongest also in early 2016 (WMO, 2017).

[3] An alarming development in view of the 2015 Paris Agreement the aim of which is to 'hold' the global average temperature increase to well below 2 0C above pre-industrial levels (UNFCCC, 2015).

Figure 4

Spatial distribution of the global temperature anomalies in 2016 (relative to the 1961-1990) (WMO, 2017)

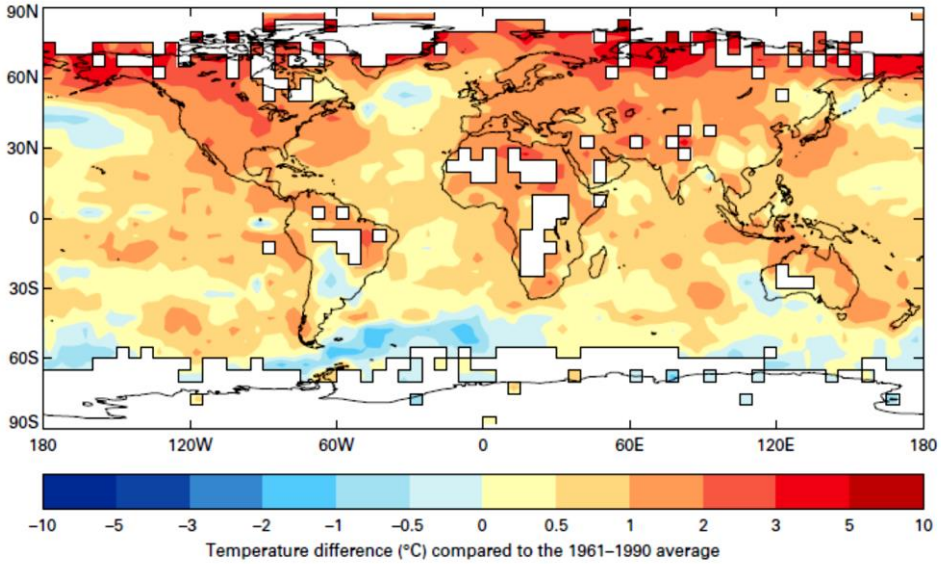

10. Climate is controlled by the heat inflows and outflows and its storage dynamics in the various constituents of the Earth System, i.e. the ocean, land and atmosphere (IPCC, 2013). Most of the heat storage occurs in the ocean, as it absorbs about 80 per cent of the heat added to the climate system and, thus, changes in ocean temperature are important indicators of climatic changes. In recent years, there has been ample evidence of ocean warming, with the rate being estimated as 0.64 Wm^{-2} for the period 1993-2008 (Lyman et al., 2010) and 0.5 - 0.65 Wm^{-2} for the period 2003-2013 (Dieng et al., 2017). Water temperature rise has been observed down to depths of 3000 m since 1961 (IPCC, 2013). There is an apparent correlation between the increase in ocean heat content and sea level rise (Fig. 5) which is the presumed to be due to steric effects/thermal expansion (NASA, 2016).

Figure 5

Global average sea level rise and change in ocean heat content for 1993-2013 Sea-level data from TOPEX (1993-2001), Jason-1 (2002-08) and Jason-2 (2008-13) ((http://sealevel.colorado.edu/). Ocean heat content (upper 700 m) relative to the 1993-2012 average. Data from CSIRO/ACE CRC, PMEL/JPL/JIMAR, NODC, and EN4.0.2 (MetOffice, 2014))

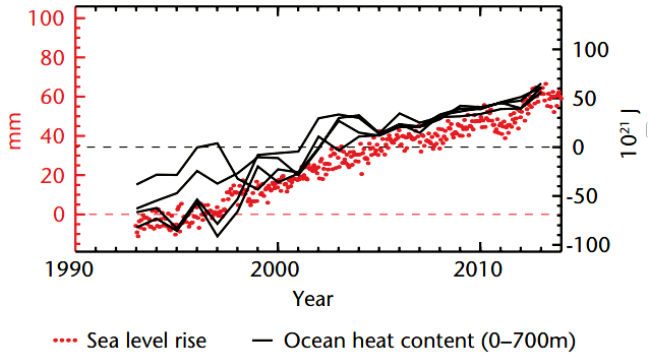

11. Analysis of global precipitation data from land areas reveal that there is an increasing trend in the twentieth century (Fig. 6), especially in middle and high latitudes

(low confidence before 1951, medium confidence afterwards). However, when the analysis includes only the NH mid-latitudes, confidence in the precipitation trends for the years after 1951 becomes high. Generally, global precipitation data show mixed long term trends (IPCC, 2013) and strong regional variability.

Figure 6

Total annual global land precipitation for the period 1901-2013 in relation to the 1901-2000 (EPA, 2015)

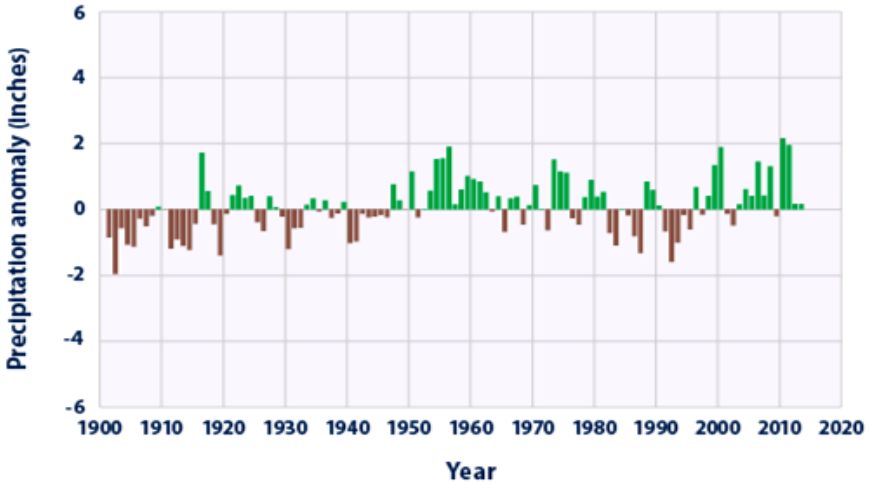

12. Heavy precipitation events have increased in intensity and/or frequency in many parts of Europe and North America, whereas there has been an increased frequency and intensity of drought events in the Mediterranean and parts of Africa (IPCC, 2013). Schneider et al. (2017) applied mean weather-dependent corrections to precipitation data from 75,100 meteorological stations (Global Precipitation Climatology Center-GPCC) and found a mean annual precipitation of about 855 mm (excluding Antarctica) for the period 1951-2000; they also suggested that a warming of about 1 ^{0}C relative to pre-industrial levels could be accompanied by a 2 to 3 per cent increase in global precipitation.

Figure 7

Differences between mean annual land precipitation for different 30-year periods (a) 1931-1960; (b) 1941-1970; (c) 1951-1980; (d) 1961-1990; (e) 1971-2000 and (f) 1981-2010 to GPCC's precipitation climatology 1951-2000 (Meyer-Christoffer et al., 2015)

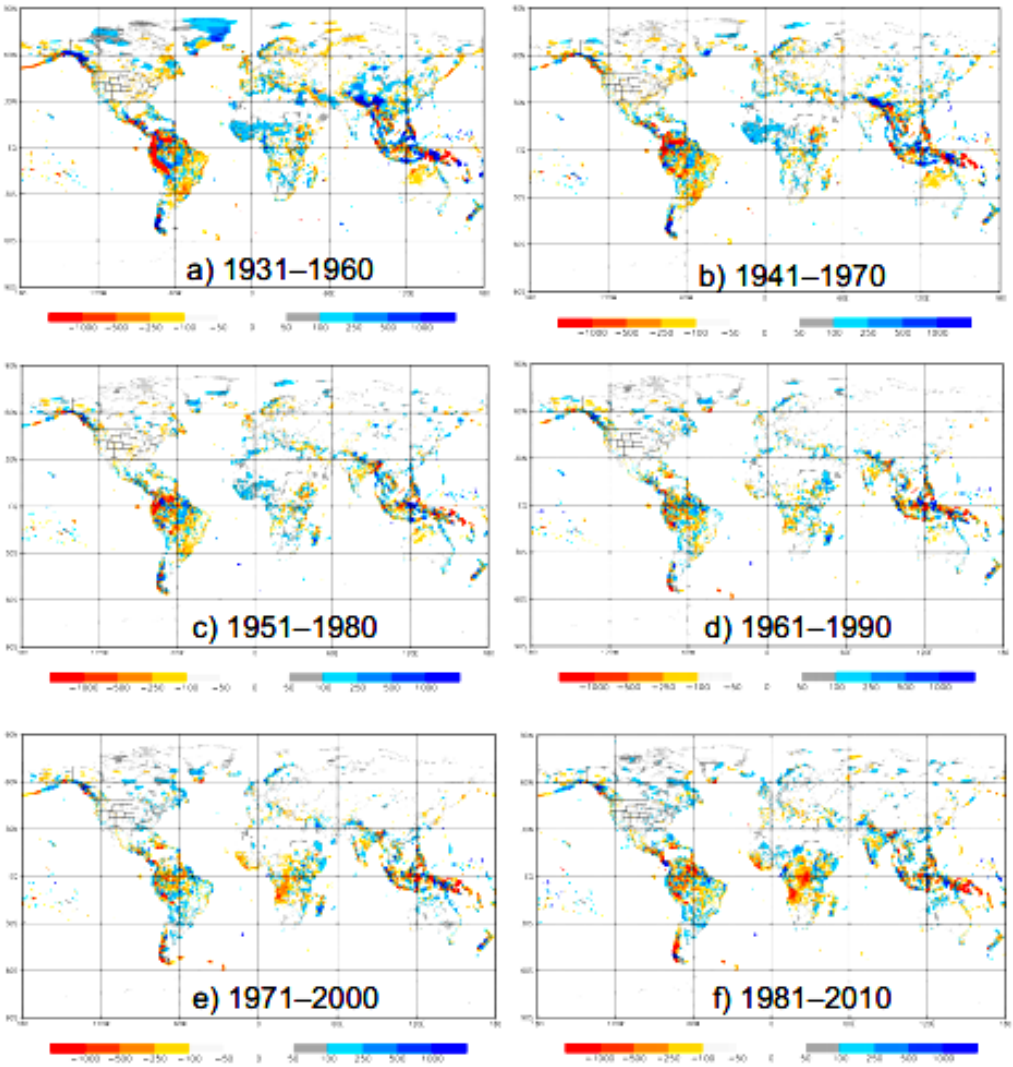

13. In the periods 1931-1960 and 1941-1970, there were larger differences compared to those in the 1951-2000 period; more rainfall occurred over West Africa and less over the SE Asia and especially Indonesia (Fig 7). In Europe and N. America, precipitation decreased in the south and increased in the north. In Spain, precipitation patterns appear to have changed substantially in the last 20 years; dry periods became lengthier, annual rainfall decreased by up to 15 per cent, and the number of heavy precipitation events decreased (Valdez- Abellan et al., 2017).

14. Precipitation decreased in the most recent 30 year periods in August, September and October, which might be related to more frequent ENSO events during the last decades and weakened Indian and Southeast Asian summer monsoons (Schneider et al., 2017). Global precipitation in 2016 was strongly influenced by the transition from El Niño conditions in the early year to neutral or weak La Niña conditions in the second half. This resulted in strong seasonal contrasts. Some regions experienced post-El Niño heavy rainfall, resulting in annual totals that were well above average. Indonesia and Australia, which were

influenced by a negative IOD, had extensive areas with rainfall above the ninetieth percentile (wettest 10 per cent of all years). It was also a wet year in many NH high-latitude areas.

1.1.2 Snow and sea ice

15. The warming trend also affects the cryosphere. Snow cover in the North Hemisphere (NH), i.e. about the 98per cent of the global snow cover, has declined by 11.7 per cent per decade in June (EEA, 2015a) over the period 1967-2012. However, this trend is not uniform. Some regions (e.g. the Alps and Scandinavia) show consistent decreases in the snow cover depth at low elevations but increases at high elevations, whereas in other regions (e.g. the Carpathians, Pyrenees, and Caucasus) there are no consistent trends (EEA, 2012). Over the past few decades, research shows a downward trend in the extent and duration of snow cover in the Arctic region.

Figure 8
Winter Snow Cover Extent in North America (left) and Eurasia (right) (NOAA 2017a)

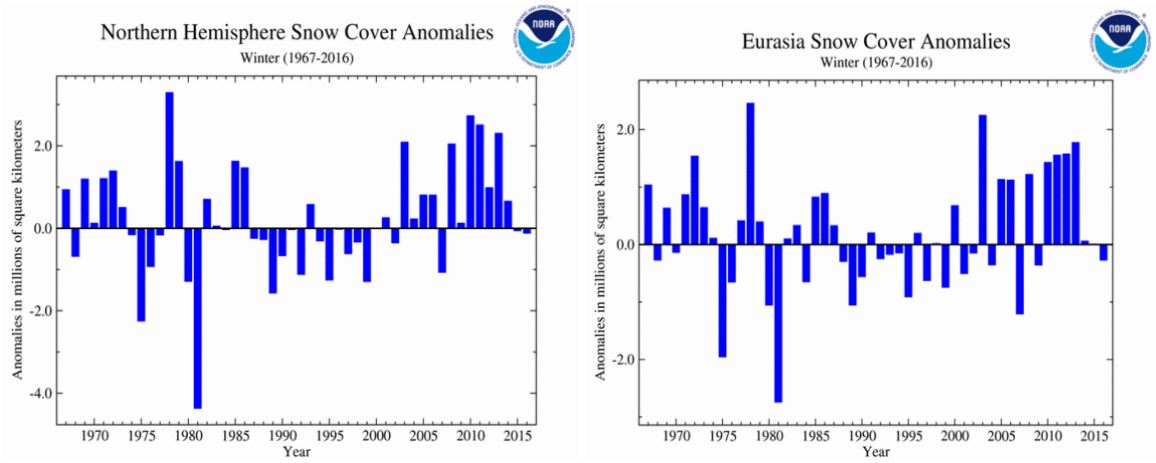

16. NH winter snow cover extent (SCE) has changed slightly in the 50-year record (NOAA, 2017a). In 2016, the winter SCE (December 2015-February 2016) was about 120,000 km^2 below the 1981-2010 average, although several winter storms moved across N. America in January 2016 increasing significantly the monthly snow cover to about 810,000 km^2 above the 1981-2010 average. (Fig. 8). In Eurasia, the winter SCE for 2015-16 was 270,000 km^2 below average. This was the smallest winter SCE since 2006/07. Similarly to North America, the Eurasian SCE was below average during December and February and above-average during January.

17. Arctic sea ice is in decline (Fig. 9). Sea ice usually expands during the cold season to a March-April maximum, and then contracts during the warm season to a September minimum; in contrast, Antarctic sea ice typically contracts during the SH warm season to a minimum extent in February-March (late summer) and expands during the cold season to a September maximum. Minimum Arctic sea ice extent has declined by about 40 per cent since 1979 and most September (minimum) records have occurred in the last decade.

Figure 9

Trend in the monthly Arctic sea ice extent in April during 1979-2017 (NSIDC, 2017)

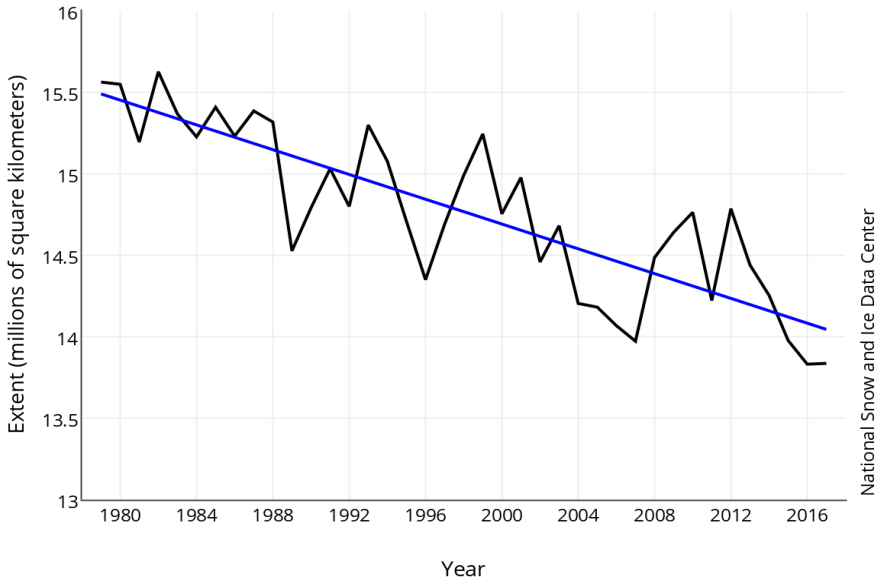

18. In November 2016, Arctic and Antarctic sea ice extents had dropped to record lows; ice conditions were so unusual, that were described as a "black swan" event (NSIDC, 2017). During each month of 2016, Arctic sea ice extent was below average. Seven months in 2016 had record lows in Arctic sea ice extent (Fig. 11). When averaged for the entire year, Arctic sea ice extent was 12.6 per cent below average.

19. The 2016 annual maximum sea ice extent in the Arctic was the lowest in the satellite record over most Arctic regions, with notable exceptions in the Labrador Sea, Baffin Bay and Hudson Bay. Maximum and minimum sea ice extent was 1.12 and 2.08 million km^2 below the 1981-2010 average, respectively. Large areas of the open ocean, which are typically ice-covered in mid-September, were observed with an ice extent minimum (e.g. large areas of the Beaufort, Chukch, Laptev and East Siberian Seas). Antarctic sea ice was near average during the first 8 months of 2016. In early September 2016, Antarctic sea ice extent began a rapid decline and was near record low levels for the rest of the year (Fig. 10).

Figure 10

Daily Arctic (left) and Antarctic (right) sea ice extent in 2016 (NOAA, 2017, data from NSIDC)

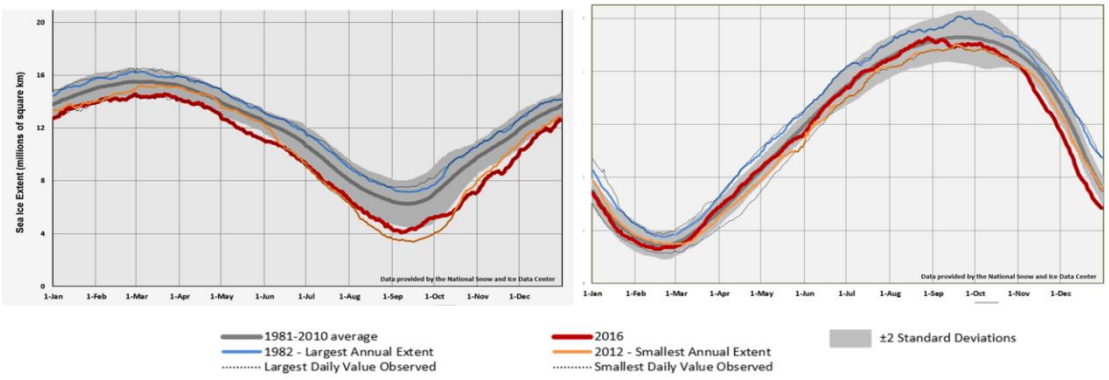

20. When averaged for the entire year, the Antarctic sea ice extent was 4.2 per cent below average, the second smallest on record. In August 2016, the Antarctic sea ice reached its maximum extent at 18.44 million km^2; this was the earliest occurrence of the maximum extent since 1979.Arctic sea ice has not been declining as rapidly in winter as it has been in summer (WMO, 2016). Greenland's ice sheet mass was measured by Velicogna et al. (2014); they found a loss of 280 ± 58 Gt $year^{-1}$, accelerating by 25.4 ± 1.2 Gt $year^{-1}$. On the same study, ice mass loss of 74 ± 7 Gt $year^{-1}$ was observed from nearby Canadian glaciers and ice caps with acceleration of 10 ± 2 Gt $year^{-1}$.[4]

1.1.3 Sea level

21. During the last decades, a significant rise of the mean sea level has been observed due to: (a) ocean thermal expansion (OTE), i.e. ocean volume changes due to steric effects; (b) glacio-eustasy i.e. ocean mass increases from the melting of the Greenland and Antarctic ice sheets (GIS and AIS) and the glaciers and ice caps (GIC); (c) glacio-isostatic adjustment (GIA); and (d) changes in terrestrial water storage (e.g. Hanna et al., 2013). The rate of global sea-level rise-SLR increased sharply above the relatively stable background rates of the previous 2000 years (e.g. Church and White, 2006; Engelhart et al., 2009; Gehrels and Woodworth, 2012; IPCC, 2013; Horton et al., 2014). Since 1860, global sea level has increased by about 0.20 m; during this period, global SLR rates averaged 1.3 to 1.8 cm per decade (Church et al., 2013; Hay et al., 2015). However, the rate of increase becomes progressively greater; there is a discernible acceleration in the global sea level since the 1900s (Fig. 11). As with temperature, the long-term upward trend in sea level has varied over the decades. For example, there were lower rates of increase during the early part of the century and much of the 1960s and 1970s; sea level increased more rapidly during the 1930s and through the 1950s. Currently, satellite and tide gauge observations suggest a global sea level rise of 3.3 ± 0.25 cm per decade since 1993 (Church et al., 2013).

Figure 11

Estimated sea level change (mm) since 1900. Data through 1992 are the tide-gauge record of Church and White (2011) with the change rate multiplied by 0.78, so as to yield a mean 1901-1990 change rate of 1.2 mm year-1 (Hansen et al., 2016)

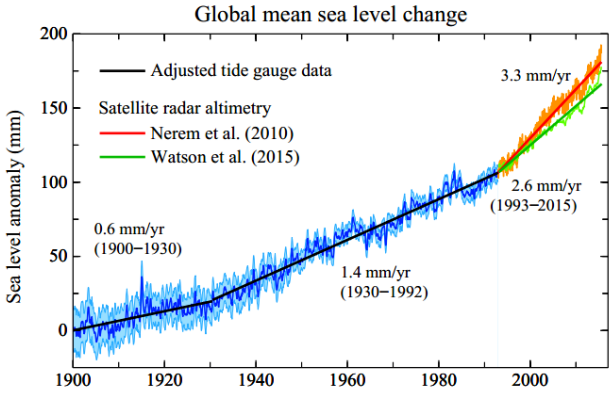

[4] These processes have had significant effects on global SLR. Observations indicate that the contribution of Greenland's ice loss has increased from 0.09 (-0.02 - 0.20) mm yr-1 in 1992-2001 to 0.59 (0.43 - 0.76) mm yr-1 in 2002-2011, while the contribution of Antarctica's ice sheet melt increased from 0.08 (-0.10 to 0.27) mm yr-1 in 1992-2001 to 0.40 (0.20 to 0.61) mm yr-1 in 2002-2011. Altogether, ice sheet melt contribution to SLR is estimated as 0.60 (0.42 - 0.78) mm yr-1 for the period 1993-2010 (IPCC, 2013).

22. Mean sea level trends and variations in regional climate have led to changes in the trends of extreme high water levels in the late twentieth century. There is considerable regional (spatial) variability in the coastal sea level rise trends (Menendez and Woodworth, 2010). In Europe, sea levels have increased along most of its coast in the last 40 odd years, with the exception of the N. Baltic coast (EEA, 2012). Some regions experience greater sea-level rise than others. In the tropical western Pacific some of the highest rising sea-level rates over the period 1993-2015 are observed, which may have been an additional contributing factor in the devastation of several areas of the Philippines during the storm surge of the typhoon Haiyan (November 2013).

1.1.4 Extreme climate events

23. Climate change is often characterized in the public discourse by the increase in global mean temperature. However, for society, economy and the environment, regional impacts and changes in extremes, such as heat waves, droughts, or floods, are generally most relevant (Vogel et al., 2017). It is essential to understand and communicate the actual implications of such events on the infrastructure/activities for a given global temperature target (Seneviratne et al., 2016). Changes in the mean climate can lead to changes in the frequency, intensity, spatial coverage, duration, and timing of weather and climate extremes, potentially resulting in unprecedented extremes. These extremes can, in turn, modify the distributions of the future climatic conditions; thus, future mean conditions for some climatic variables are projected to be located within the 'tails' of the present conditions (IPCC, 2013).

24. Extreme events (e.g. storms, floods, droughts and heat waves) as well as changes in the patterns of particular climatic systems (e.g. the monsoons) (King et al., 2015) can be, at smaller spatio-temporal scales, the most impacting climatic phenomena, since they may induce abrupt and more severe effects/natural disasters than changes in the mean variables. Moreover, societies are rarely prepared to face efficiently extreme weather events, having become dependent on predictable, long-term climatic patterns (MetOffice, 2014). In USA, extreme hydro-meteorological event events cause on average about 650 deaths and $15 billion in damages annually and are responsible for some 90 per cent of all declared by the President disasters. In addition, about one-third of the economy (around $3 trillion) appears to be sensitive to weather and climate; since 1980, the USA has sustained 208 hydro-meteorological disasters with a total cost exceeding $1.1 trillion (NOAA, 2017c).

25. Many indicators of climate extremes showed changes consistent with warming, including a widespread reduction in the number of frost days in mid-latitude regions and discernible evidence that warm extremes have become warmer and cold extremes less cold in many regions (IPCC, 2013). Evidence suggests a general change in the frequency of high impact temperature and precipitation extremes over land, irrespective of the type of dataset and processing method used (MetOffice, 2014). A slight global mean decrease in the annual number of mild days (i.e. days with maximum temperature between 18-30 ^{0}C and precipitation < 1 mm) is projected in the near future (4 days/year for the 2016-2035 period and 10 days/year for the 2081-2100 period) (Van der Wiel et al., 2017).

26. Extreme events have consequences that are difficult to predict. Their variability covers a large spectrum, such as sudden and transient temperature changes, rapid retreats of sea ice, bouts of abnormally high precipitation, intensive storms, storm surges, extended droughts, heat waves and wildfires and sudden water releases from melting glaciers and permafrost slumping that may have substantial and costly impacts on infrastructure. In addition, there is evidence to suggest that extreme events, such as tropical and temperate storms, may respond to a warming climate by becoming even more extreme (Emanuel, 2005; Ruggiero et al., 2010; WMO, 2014; MetOffice, 2014). For example, even a modest increase (of 5 m/s) in the surface wind speed of the tropical cyclones driven by a 1 °C rise

in the ocean temperature might result in a substantial increase of the incidence of the most intense and destructive (Category 5) cyclones (e.g. Steffen, 2009). The implications of these extreme events for e.g. the coastal communities and infrastructure could be severe, as they may increase the likelihood of extreme sea levels (ESLs) from storm surges and waves (e.g. Stockdon et al., 2012) and consequently of coastal floods, especially if combined with the projected increases in the mean sea level (Hallegate et al., 2013).

27. In addition, increases in the intensity and frequency, and/or changes in the patterns, of extreme waves (e.g. Ruggiero, 2013; Bertin et al., 2013; Mentaschi et al., 2017) will also induce, at least temporarily, coastal erosion or inundation, particularly when combined with increasing mean sea levels (e.g. Losada et al., 2013; Vousdoukas et al., 2017). Storm surges pose a particular threat to highly developed coastal areas, particularly the low lying coasts such as the Rhine, Danube and the Mississippi river deltas which are considered hotspots of coastal erosion/vulnerability due to their commonly high relative mean sea level rises (ECE, 2013). In Southern Europe, analysis of the extreme coastal sea level/storm surges recorded by tide gauges has shown that changes in extreme water levels tend to be dominated by the mean sea level rise (e.g. Marcos et al., 2011). Coastal areas currently experiencing erosion and/or inundation are projected with high confidence that will continue to do so in the future, due to increasing sea levels, all other contributing factors being equal (Hallegatte et al. 2013; Vousdoukas et al., 2017). The projected rise in extreme sea levels (ESLs) constitutes a serious threat to global coastal societies. Their safety and resilience depends on the effectiveness of natural and man-made coastal flood protection, i.e. the capacity of the coast to act as a buffer and absorb ocean energy through wave shoaling and breaking processes (e.g. Vousdoukas et al., 2012).

Figure 12

Future changes in heavy rainfall in the 12 km (left) and 1.5 km (right) resolution models, for winter (top) and summer (bottom)

(Both models show increased hourly rainfall intensity during winter, but the 1.5 km model also reveals significant increases in short-duration rain intensity during summer. Changes are for 2100 under the high emission scenario RCP8.5 (Met Office, 2014))

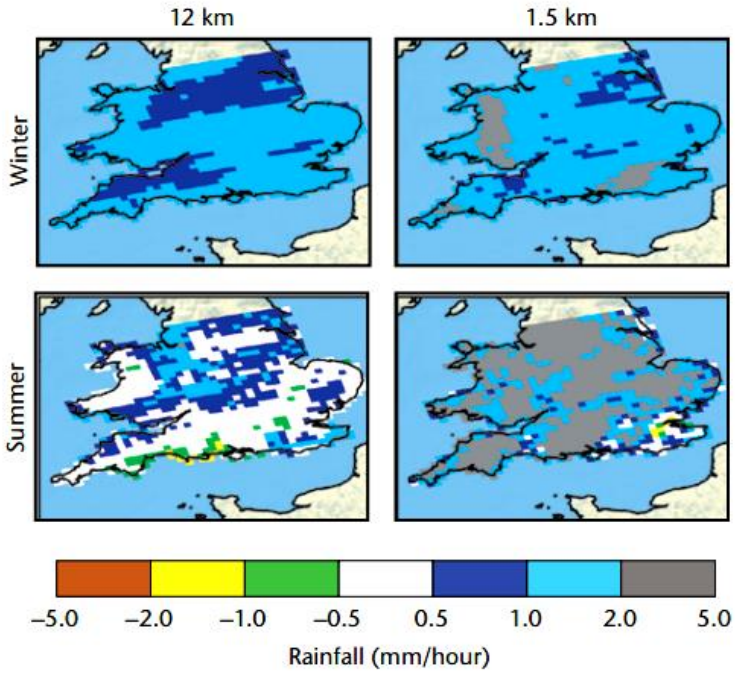

28. One of the clearest trends appears to be the increasing frequency and intensity of heavy downpours; this increase has been responsible for most of the observed increases in overall precipitation during the last 50 years. Projections from climate models suggest that these trends will continue during this century (Karl et al., 2009). A fine resolution model (MetOffice, 2014) projected that whereas UK summers are to become drier by 2100, summer downpours will be heavier (Fig. 12). It is likely that the frequency of such events will increase over many regions in the twenty-first century, especially in the high and tropical latitudes and the northern mid-latitudes in winter. Heavy precipitation events are also predicted with medium confidence to increase even in regions with projected decreases in the total precipitation (ECE, 2013).

29. River flooding is the most serious and widespread weather hazard (King et al., 2015). Between 1980 and 2014 river floods accounted for 41 per cent of all loss events, 27 per cent of fatalities and 32 per cent of losses (Munich Re, 2015). Riverine floods involve both physical and socio- economic factors. The former depend on the hydrological cycle, which is influenced by changes in temperature, precipitation and glacier/snow melts, whereas the latter by land use changes, river management schemes, and flood plain construction (EEA, 2010). In the ECE region, floods are an ever present threat.

30. The current trends in the Eurasian countries show a significant flood hazard (for the 1 in a 100-year events), particularly for central and eastern Europe, the central Asia and along the large S-N drainage basins of Siberia (Fig. 13). However, changes in extreme hydrological events and their impacts are better studied at a regional/local scale, with most existing studies focusing on the generation and impacts of floods due to e.g. increases in torrential precipitation. In Europe, annual water discharges have generally been observed to increase in the north and decrease in the south (EEA, 2012), a trend that is projected to hold in the future, as is associated with projected changes in precipitation (EEA, 2015c). By the 2050, there is at least a 50 per cent chance that climate change alone would lead to a 50 per cent increase in flooded people across sub-Saharan Africa, and a 30 to 70 per cent chance for such an increase in Asia; by 2100 the risks have been projected to be greater (King et al., 2015).

Figure 13

Current flood hazard (95 per cent probability) in the Eurasian region of the ECE for the 100-year flood from a global GIS model based on river discharge time-series

(DEM resolution 90 m. Areas over 60 ^{0}N are not fully covered (From UNEP-GRID and UNISDR, 2008). (ECE, 2013))

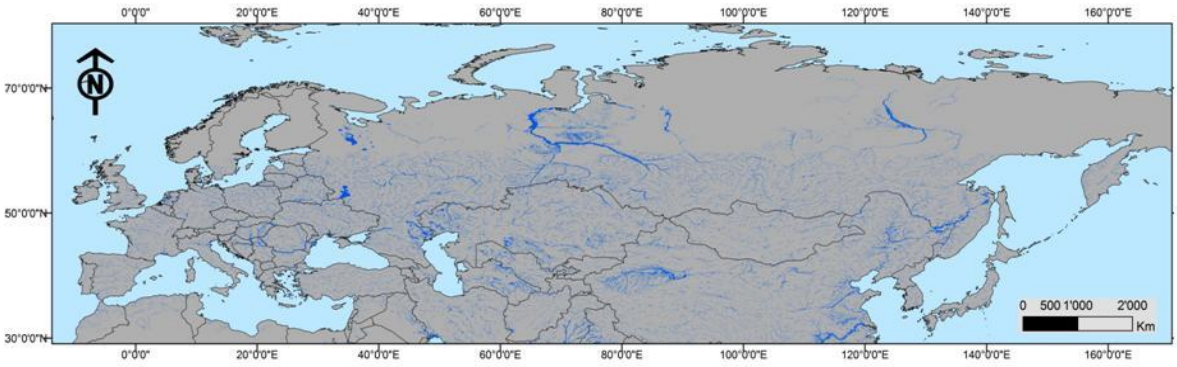

31. Slope failures/landslides are also expected to increase at mountainous areas, as are also linked to heavy downpours (e.g. Karl et al., 2009). Consequently, flood damages in e.g. Europe are expected to rise considerably by the end of the century, being generally higher in the north than in the south (Alfieri et al. 2015). There is also evidence to suggest increases in the frequency and intensity of heat waves (e.g. Beniston and Diaz, 2004; IPCC,

2013); generally, there has been a 3-fold increase since 1920s in the ratio of the observed monthly heat extremes to that expected in a non-changing climate (Coumou and Rahmstorf, 2012). At a global scale, with mean temperatures continuing to rise, models project that increases in the frequency/magnitude of hot days and nights and decreases in the cold days and nights are virtually certain (IPCC, 2013). Since 1950s, it is very likely that there has also been an overall decrease in the number of unusually cold days and nights and an overall increase in the number of unusually warm days and nights at the global scale (for land areas with sufficient data). For example, most of North America appears to have experienced more unusually hot days and nights, fewer unusually cold days and nights and fewer frost days (ECE, 2013). Heat waves are often associated with severe droughts (as e.g. the European summer 2003 heat wave). Generally, droughts are becoming more severe in some regions, a trend that is projected to hold (and possibly increase) in the twenty-first century (IPCC, 2013).

1.1.5 The 2011-2016 period

Temperature and precipitation

32. The last 6-year period (2011-2016) has been the warmest on record. Temperatures were more than 1 ^{0}C above the 1961-90 average (over most of Europe, northern Asia and the southwest US) and reaching about 3 ^{0}C above average in regions of the Russian Arctic. 2016 was the warmest year on record (1.1 ^{0}C higher than the 1901-2000 average of 14.0 ^{0}C), surpassing the previous records of 2015 and 2014, with the average land surface temperature at record high (Fig. 14).

33. In 2016, the global average temperature was 0.83 ± 0.10 ^{0}C warmer than the average for the 1961-1990 reference period and about 1.1 ^{0}C above the pre-industrial period. It was the warmest year on record for both land and oceans and for both hemispheres. The 5-year mean temperatures also reached their highest values on record, with the 2012-2016 period being 0.65 ^{0}C above the 1961-1990 average. Global temperatures continued to be consistent with a warming trend of 0.1 °C to 0.2 ^{0}C per decade (WMO, 2017). Nearly all of Eurasia was much warmer than average. Noteworthy were also the seasonal anomalies: the warmest springs on record were observed in N. America (2012) and Europe (2014), whereas the hottest summer on record for N. America was in 2012. The year 2015 was the first time the global average temperatures were 1 ^{0}C or more above the 1880-1899 average, a trend that continued in 2016 (NOAA, 2017b). Globally, may of the warmest years have occurred since 1998 (Fig. 14).

34. Phenomena, such as El Niño (or La Niña) that can warm or cool the tropical Pacific Ocean, may be responsible for short-term variability in the global temperature. An El Niño event occurred in 2015 and the first part of 2016. Research suggests direct impacts of the 2015/2016 El Niño; warming in the tropical Pacific (Fig. 15) increased the annual global temperature anomaly for 2016 by almost 0.1 ^{0}C (NOAA, 2017b).

35. Sea surface temperatures (SSTs) for the period were above average in most of the oceans, with the exception of some areas in the Southern Ocean and the eastern South Pacific. Warm temperatures also occurred in the subsurface, with the integrated ocean heat content within the 0-700 m layer being higher in 2013 and 2014 than any previous time according to 5 different data sets (NOAA, 2016). There were two notable ocean temperature anomalies in late 2013: (i) a large area of very warm water (> 2 ^{0}C above average) in eastern North Pacific; and (ii) a persistent pool of water exhibiting SSTs below-normal in eastern North Atlantic.

Figure 14

The 2011-16 period was the warmest period on record, with temperatures 0.57 ^{0}C above the 1961-1990 average and 0.51 ^{0}C above the 2006-2010 average. Land temperatures were > 1 ^{0}C above the 1961-90 average over most of Europe, the southwestern US and the Asian sector of the Russian Federation and most areas to the north of 60 ^{0}N (NOAA, 2017b).

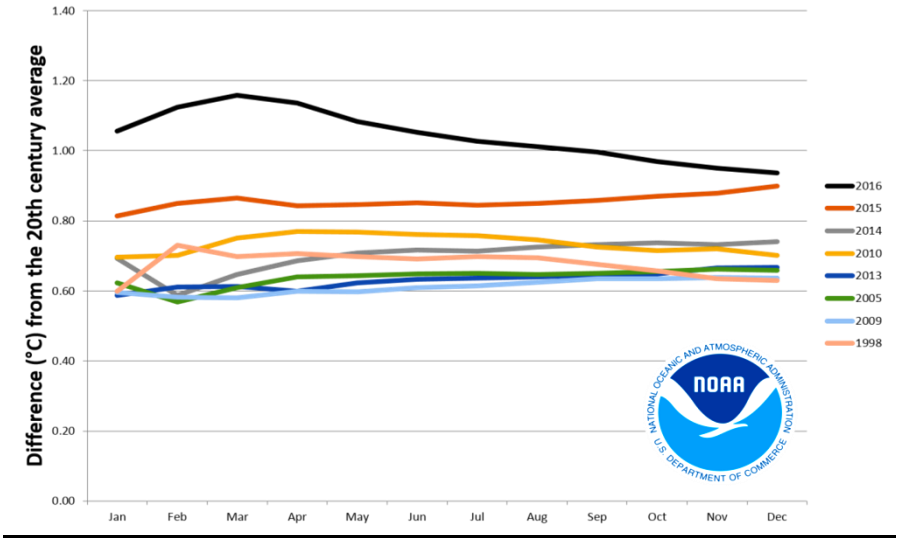

36. Land precipitation was strongly influenced early and late in the 2011-2016 period by the El Niño-Southern Oscillation (ENSO), with La Niña conditions for much of 2011 and early 2012, and a strong El Niño at the 2015-early 2016. 2011 was assessed by NOAA as being the world's second-wettest year on record, with 2012, 2013 and 2014 all close to the long-term average. A major feature of the 6-year period is the presence of persistent multi-year rainfall anomalies over several regions, most of which began after the end of the 2012 La Niña. In 2016, global precipitation was strongly influenced by the transition from El Niño conditions in the early year to neutral or weak La Niña conditions in the second half of the year. This resulted in strong seasonal contrasts (but annual totals close to the average conditions) in many regions. In other regions, however, heavy rainfall occurred in the post-El Niño period, resulting in annual totals well above average (WMO, 2017).

37. Three regions (eastern half of Brazil, western US, and parts of eastern Australia) had large areas in which rainfall for October 2012-September 2015 was below the 10th percentile, whereas there were also regions where precipitation exceeded the 90th percentile (e.g. in eastern Russia). Regarding Europe, there was a marked north/south split, with very wet conditions in Scandinavia and very dry conditions in much of the central and SE Europe. Major annual precipitation anomalies were less common in the years 2012-2014, with significant anomalies observed in NE Europe, parts of China and Argentina (2012) and SE Europe (2014); in the ECE region, very dry conditions occurred over much of the central US and central (2012) and western Russia (2014).

Figure 15
Temperature anomalies in 2016 (JMA, 2017)

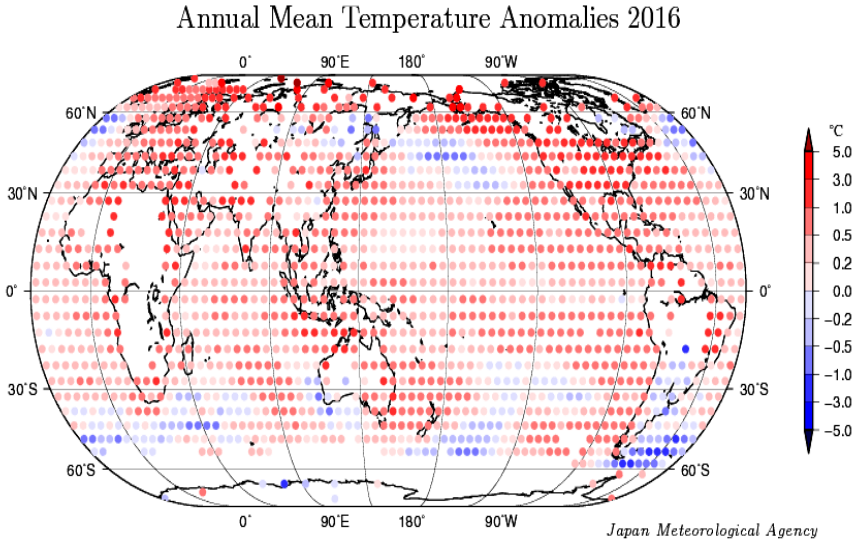

The circles indicate temperature anomalies from 1981-2010 baseline averaged in 5°x 5° grid boxes.

38. 2016 was a wet year in many high-latitude NH areas. Precipitation above the 90th percentile was observed in a large swath extending from Kazakhstan across the western Russian Federation into Finland, northern Sweden and Norway. However, large areas of the northern-central Russian Federation were dry, with much of the region between the Urals and Lake Baikal and to the north of 55 ^{0}N having precipitation below the 10th percentile. The tropical west coast of S. America, which normally experiences heavy rains during strong El Niño years, had only patchy rainfall in early 2016 (seasonal rainfall generally close to average). Another non-typical region was California, where the 2015-2016 seasonal rainfall was near average (after 4 very dry years), increasing towards the end of the year.

39. Precipitation was close to average over most of central and western Europe, with a very wet first half and a dry second half of the year. The 2015/2016 winter was wet across the western Europe, with the UK having its second-wettest year. May and June were also very wet in western and central European regions, causing significant flooding in France and Germany. However, the July-September period was dry, with France having its driest July/August on record. December was also extremely dry, with many areas having less than 20 per cent of normal precipitation. Lowland Switzerland had its driest December and third driest month on record. One particular example of the high variability in the precipitation of 2016 was at Belgium; Uccle had its wettest January-June on record (62 per cent above average), followed by its third-driest July-December (36per cent below average) (WMO, 2017).

CASE: February 2016, the warmest February since records began

Average land/ocean surface temperature for February 2016 was the highest for February since records began, at 1.21 °C above the twentieth century average of 12.1 °C (surpassing the previous record set in 2015 by 0.33°C) (NOAA, 2016d). Overall, the 6 highest monthly temperature departures in the record have all occurred in the period September 2015-February 2016.

A vast NH region stretching from central Russia into Eastern Europe (as well as Alaska) showed February temperatures more than 5 °C above the 1981-2010 average. A few pockets in Asia were cooler than average, including part of Far East Russia.

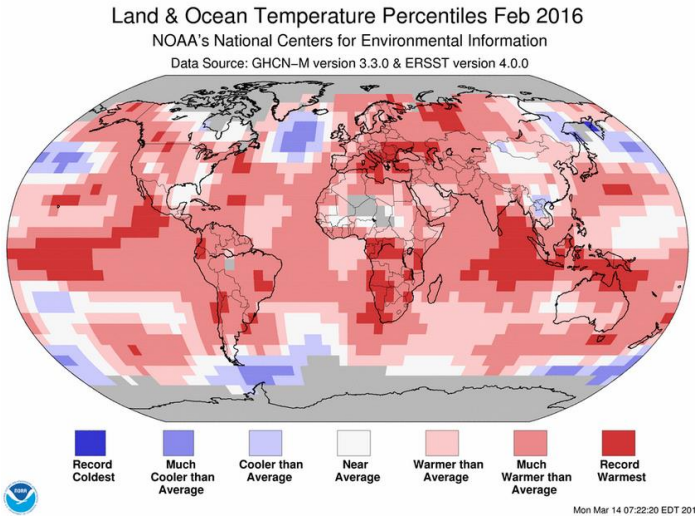

Land/Ocean Temperature anomalies for February 2016 compared to the global average (NOAA, 2016d)

Snow and ice

40. The cryosphere component of the Earth system includes solid precipitation, snow cover, sea ice, lake and river ice, glaciers, ice caps, ice sheets, permafrost and seasonally frozen ground. The cryosphere provides some of the most useful indicators of climate change, yet is one of the most under-sampled domains of the Earth system. There are at least 30 cryospheric properties that should be (ideally) measured. Many of these properties are measured at the surface, but spatial coverage is generally poor. However, some of these properties have been measured for years from space. The major cryosphere elements for which assessment is provided for 2016 include snow cover, sea ice, glaciers and ice sheets.

41. Despite the overall high temperatures of the 6-year period, there were still episodes of abnormal cold and snow in the NH. A prolonged period of extreme cold affected Europe in February 2012. It was the worst cold spell since 1985 or 1987 in many areas of the central and western Europe, with temperatures remaining below 0 ^{0}C continuously for 2 weeks or more in most of central Europe, although no low temperature records were set. This event also brought extremely heavy snow in some places, especially in parts of eastern Italy. March 2013 was also notably cold in much of Europe with significant blizzards in places. The winters of 2013-14 and 2014-15 were both significantly colder than normal in many central and eastern areas of the US and southern Canada, with persistent low temperatures over the region for extended periods (although no records were set). The cold was especially persistent in February 2015, when temperatures in Montreal, Toronto and Syracuse did not rise above 0 ^{0}C. In coastal regions there were frequent snowfalls, resulting in Boston experiencing its greatest seasonal snowfall on record (WMO, 2016).

42. Northern hemisphere mean annual snow cover extent for 2016 was 24.6 million km^2, 0.5 million km^2 below the 1967-2015 average; this was very similar to 2015 (see also Fig. 8). After above-average snow cover in January, snow cover was well below average from February to June, with cover between 2.4 million km^2 and 3.3 million km^2 below average. The April mean snow-cover extent was the lowest on record, with March ranking second, February and June third and May fourth. Autumn snow cover, however, was above average, as it had been in the previous three years. There were positive anomalies from September and each month from October to December. There are no comparable snow-cover records for the southern hemisphere, where (except for the Antarctic) snow is generally rare outside high mountain regions. In Australia, peak seasonal snow depths at Spencers Creek in the Snowy Mountains were slightly below average, but high precipitation and below-average temperatures in September and October led to a late finish to the season (WMO, 2017).

43. Arctic sea-ice extent was well below average in 2016 and at record low levels for large parts of the year. The seasonal maximum of 14.52 million km^2 (on the 24 March) was the lowest seasonal maximum in the 1979-2016 satellite record (Fig. 16), just below that of 2015. Sea-ice extent again dropped to record lows in May and June but a relatively slow summer melt resulted in a seasonal minimum (4.14 million km^2) being above the 2012 record. The 2016 autumn freeze was slow. The mean November extent of 9.08 million km^2 was 0.8 million km^2 below the previous record low. Antarctic sea-ice extent was close to the 1979-2015 average for the first 8 months of 2016, reaching a seasonal maximum of 18.44 million km^2 in late August; this was the earliest seasonal maximum on record. The spring melt was exceptionally rapid, resulting in a November mean extent of 14.54 million km^2, by far the lowest on record (1.0 million km^2 below the previous record). The reasons behind the collapse of the sea ice in late 2016 are not yet understood, although local winds might have been a factor (WMO, 2017).

Figure 16

(a) September sea-ice extent for the Arctic and (b) September sea-ice extent for the Antarctic: Percentage of long-term average of the reference period 1981-2010 (Source: prepared by WMO, data from the US National Snow and Ice Data Center) (WMO, 2017)

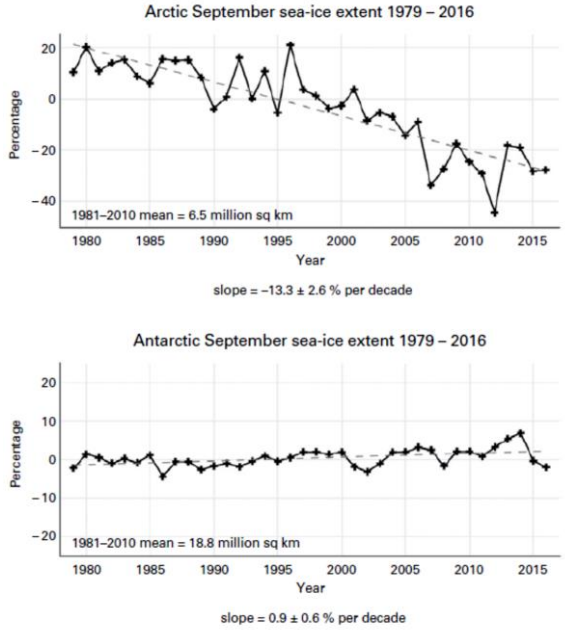

44. With Arctic and Antarctic sea-ice extent at record low levels, global sea ice extent in November was also far below average. After being more than 1 million km^2 below the 1979-2015 average for most of the year, it dropped to more than 4 million km^2 below average in November - an unprecedented anomaly - before a slight recovery in December.

45. During the last years (2011-2016), Arctic sea ice continued a decline that exceeded the 1981-2010 mean value, particularly for the winter maximum. In comparison, ice extent in the Southern Ocean reached 20.16 million km^2 in September 2014, 1.45 million km^2 above the 1981-2010 average and the highest extent in the satellite record. An abnormally slow winter freeze in 2015 resulted in sea ice extent returning to near-average levels in spring (maximum in early October of 18.83 million km^2, only 0.7 per cent above the 1981-2010 average (WMO, 2017).

46. Mountain glaciers also continued their decline during the last years, while there was also warming down to 20 m depth in Arctic permafrost regions. Permafrost temperature has increased in most regions by up to 2 ºC since 1980, leading to significant infrastructure damage; thickness of the NH permafrost has decreased by 0.32 m since 1930 (IPCC, 2013). Snow cover extent was also well below average in the period 2011-2016. In the NH, anomalies in the snow cover extent showed strong seasonal variability, but the overall mean extent in the 5-year period was close to the 1981-2010 average. The highest seasonal anomaly occurred in the winter 2013, when snow cover extent was well above normal through the winter (WMO, 2014).

47. Data from the World Glacier Monitoring Service indicate that mountain glaciers continued to melt in 2016. Reference glaciers for which 2015/2016 data are available show a mean mass balance of -858 mm, with only one of 26 glaciers showing a positive mass balance. This mean mass balance deficit is less extreme than that of 2014/2015, but above the 2003-2015 average. The loss of Greenland ice sheets in the 12 months to August 2016 had a similar rate to that of recent means. The surface mass balance for this period was

close to the 1990-2013 average, with above-average accumulation during the colder months being offset by above-average melting in summer. The loss of glacier area was the largest since 2012 (WMO, 2017).

Sea level rise

48. In 2011-2016, mean sea level continued to rise. The period began with global sea level about 10 mm below the long-term trend (probably due to the strong La Niña); however, by mid-2012, mean sea level trend had rebounded. A marked rise occurred in early 2015 (as the 2015/2016 El Niño developed), with sea levels being of about 10 mm above the long-term trend.

49. SLR rend over the full satellite record (1993-2015, 3 mm $year^{-1}$) has been considerably higher than the average of the 1900-2010 (1.7 mm $year^{-1}$). There is evidence suggesting that the contribution to SLR from the continental ice sheet melt (particularly from those of Greenland (GIS) and west Antarctica (WAIS)) has been increasing. The contribution of GIS melting to global SLR in the 2011-13 period (that includes the extreme melt year of 2012) was approximately 1.0 mm/year, well in excess of the 0.6 mm $year^{-1}$estimated for the period 2002-2011 (IPCC, 2013).

50. Regarding the Pacific Ocean, strong regional differences were apparent in 1993-2014; these have been attributed to El Niño and La Niña events. The western Pacific has shown the world's fastest SLR rates over this period (> 10 mm $year^{-1}$ in places), compared to the eastern Pacific. Sea level rise has been more consistent in the Atlantic and Indian Oceans with most areas in both oceans showing rates similar to the global average. Global sea levels rose strongly during the 2015/2016 El Niño, rising about 15 mm between November 2014 and February 2016, well above the post-1993 trend of 3 mm $year^{-1}$.

Extreme events in the 2011-2016 period

51. In 2011-2016 there have been many extreme weather and climate events such as heat and cold waves, tropical cyclones, floods, droughts and intense storms. Several of these events caused significant damage/losses, as e.g. the 2011 SE Asian floods, the Hurricane Sandy in the Caribbean and the US (2012), droughts in the southern and central US (2012 and 2013), and floods in central Europe in May-June 2013 (Fig. 17).

Figure 17

Flood damages on European roads in June 2013: (a) Highway 8 in Grabenstaett, S. Germany ((Matthias Schrader, AP); (b) Tyrol, Austria (Kerstin Joensson, AP)

52. Fortunately, human loss does not follow the upward trend in economic losses (Fig. 18). In terms of casualties, flash floods in southern Brazil and SE Asia caused 1,700 deaths (2011), whereas Typhoon Haiyan (Yolanda) in the Philippines and floods in N. India resulted in 13,600 deaths (2013). More than 3,700 people lost their lives from heat waves in India and Pakistan (May-June 2015). The most lethal extreme event has been the 2010-

2011 drought in the horn of Africa that may have been the cause of the late 2010-early 2012 Somalia famine that was responsible for 258,000 excess deaths (WMO, 2016).

Figure 18
Human losses (left) and economic losses by decade
(Economic losses in US$ billions, adjusted to 2013 (NOAA, 2017c))

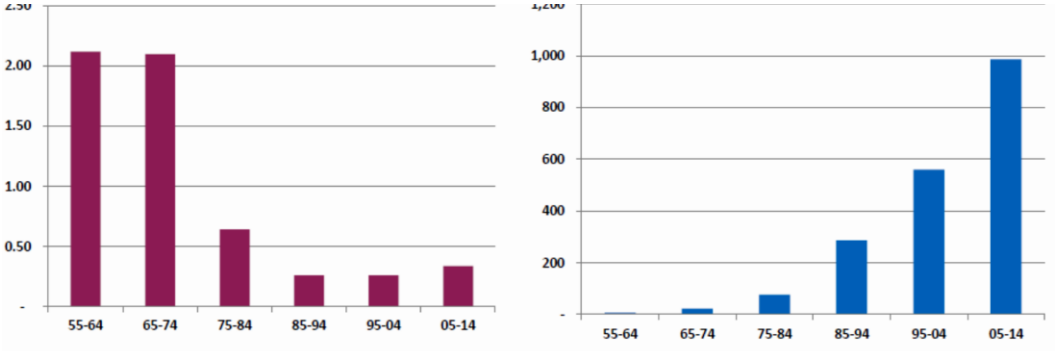

53. Generally, the 1980-2016 average has been 5.5 US$ billion disaster events (CPI-adjusted) per year, with the annual average for the most recent 5 years (2012-2016) being 10.6 such events (NOAA, 2017c).

54. Significant heat waves have been recorded in Europe during the summers of 2012, 2013 and 2014. In Austria, it was the first time that temperatures reached 40 ^{0}C or above. A prolonged heat wave affected many parts of eastern Asia in July-August 2013. The most intense heat waves of the period were recorded in May and June 2015 in India and Pakistan, during the pre-monsoon periods; temperatures were at, or above 45 ^{0}C. In western and central Europe, the most significant heat wave since 2003 was recorded in the first fortnight of July 2015, with Spain, France and Switzerland breaking all time temperature records; a few weeks later, temperatures of 40.3 ^{0}C were also recorded in Germany.

55. Severe droughts have occurred in the period 2011-2016. N. America (US and N. Mexico) has experienced severe droughts in 2011, 2012 and 2013. In July 2012, 64.5 per cent of the US territory was classified as experiencing droughts, the largest areal extent since the 1930s. Total rainfall in 2011-2016 was also 30 per cent below normal, resulting in total economic losses of approximately US$60 billion. Significant long-term droughts also occurred in Australia and southern Africa, whereas the Indian monsoon rainfall (June-September) was about 10 per cent below normal in both 2014 and 2015. In April and May 2016, India experienced a major heat wave. A record high temperature of 51.0 ^{0}C was set in the town of Phalodi. 160 people died and 330 million were affected.

56. High winds and tornadoes caused major destruction. The number of cyclones characterized by high intensity winds increased during the 6-year period. The Northwest Pacific was particularly active in 2013 and 2015, and the North Atlantic in 2011. US had one of its most active tornado seasons on record in 2011, where the total number of tornadoes ranked as the third highest on record. In 2012-2015, however, tornado activity was below the 1991-2010 average. Regarding hurricanes, Hurricane Sandy affected the Caribbean and the east coast of the United States in October 2012 causing major damage, i.e. severe coastal flooding and high record water levels and inundation (IPCC, 2013). There were 233 deaths in the US and the Caribbean whereas total economic losses were estimated as US $67 billion. Tropical cyclones had also major impacts in Asia (e.g. Typhoon Haiyan (Yolanda) and Washi (Sendong)), whereas cyclone Patricia was extremely intense with recorded wind speeds up to 322 km/h at Mexico.

57. During this period, several windstorms associated with extra-tropical cyclones occurred in Europe. In 2013, Denmark experienced the highest recorded wind (53.5 m/s)

that caused excessive damages (also in the UK, France, Germany, Netherlands and Sweden). The highest storm surge levels since 1953 were recorded in Netherlands and the UK in this period. In the 2013-2014 winter, a sequence of storms led to the UK having its wettest winter on record, causing also significant wind damage and coastal erosion (WMO, 2016).

58. In 2016, severe thunderstorms and tornadoes triggered significant losses in many parts of the world. The worst single incident occurred in Yancheng, Jiangsu province, China, when a tornado was associated with 99 deaths. It was one of the most destructive tornadoes in recorded Chinese history, at a time when the region was also experiencing severe flooding. Tornado activity in the United States was below the long-term average for the fifth consecutive year, with a preliminary count of 985 tornadoes, about 10 per cent below the post-1990 average. There were, however other severe thunderstorms. Two major hailstorms in Texas resulted in combined damage of more than US$5 billion. A notable hailstorm occurred in Brabant (Netherlands), with losses estimated at €500 million. Flash floods occurred in many parts of the NH, with notable episodes in Houston (Texas) and Tunisia. Unusually early heavy snowfalls affected Scandinavia in early November. Significant early snowfalls also affected Japan, with Tokyo receiving its first measurable November snow since records began in 1875 (WMO, 2017; NSIDC, 2017).

1.1.6 Forcing mechanism

59. A major cause of the observed increase of the heat content of the planet is considered to be the increasing concentrations of atmospheric greenhouse gases (GHGs). These gases enhance the "greenhouse effect", which is a well-documented and understood physical process of the Earth System, known since the nineteenth century (e.g. Canadell et al., 2007). Changes in the atmospheric GHG concentration affect the magnitude of the Greenhouse Effect. Water vapour is an abundant GHG and makes the greatest contribution to the 'natural' effect. Human activities have not yet shown to have had a significant direct effect on net global flows of water vapour to/from the atmosphere (e.g. Richardson et al., 2009), although locally they may have influenced such flows through e.g. deforestation and large irrigation schemes. Nevertheless, as the ability of the atmosphere to retain water vapour is strongly dependent on temperature, atmospheric water vapour is regulated by the Earth's temperature, increasing with global warming. Thus, water vapour not only follows, but also exacerbates changes in global temperature that are induced by other causes, such as the increasing concentrations of the other GHGs (e.g. Richardson et al., 2009).

Figure 19

Total annual anthropogenic GHG for the period 1970-2010 (IPCC, 2014)

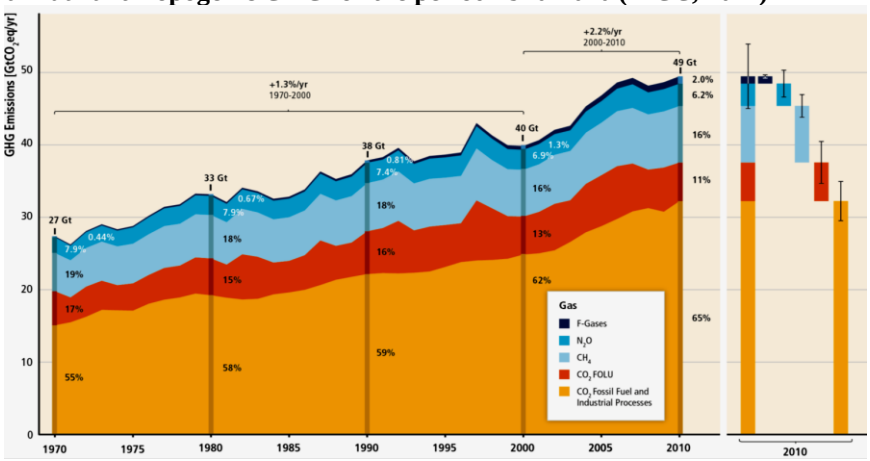

60. GHGs in the atmosphere absorb heat reflected back from the Earth's surface and, thus, store more heat in the ocean, land and atmosphere. Without the greenhouse effect, average temperatures on Earth would be about -19 °C (i.e. about 34 °C colder than it is at present). All planets with heat absorbing gases in their atmosphere, experience a Greenhouse Effect. For example, the extreme surface temperature (about 440 °C) of Venus is explained by the high concentration of GHGs in its atmosphere. The observed increase in the Earth's heat content is probably (at least partly) due to the increasing atmospheric concentrations of greenhouse gases (GHGs), that absorb heat reflected back from the Earth's surface (IPCC, 2013).It appears that the atmospheric concentrations of CO2, CH4 and the other GHGs have increased very substantially over recent decades, probably as a result of human activities (e.g. Caldeira, 2009). There is mounting evidence for a link between GHGs concentration and climate. For example, co-variation of CO2 concentration and temperature in Antarctic ice-core records suggests a close link between CO2 and climate during the Pleistocene ice ages, the exact nature of which is, nevertheless, unclear (e.g. Shakun et al., 2012).

Figure 20

Total anthropogenic GHGs in 1970, 1990 and 2010 by economic sector and country income groups (IPCC, 2014)

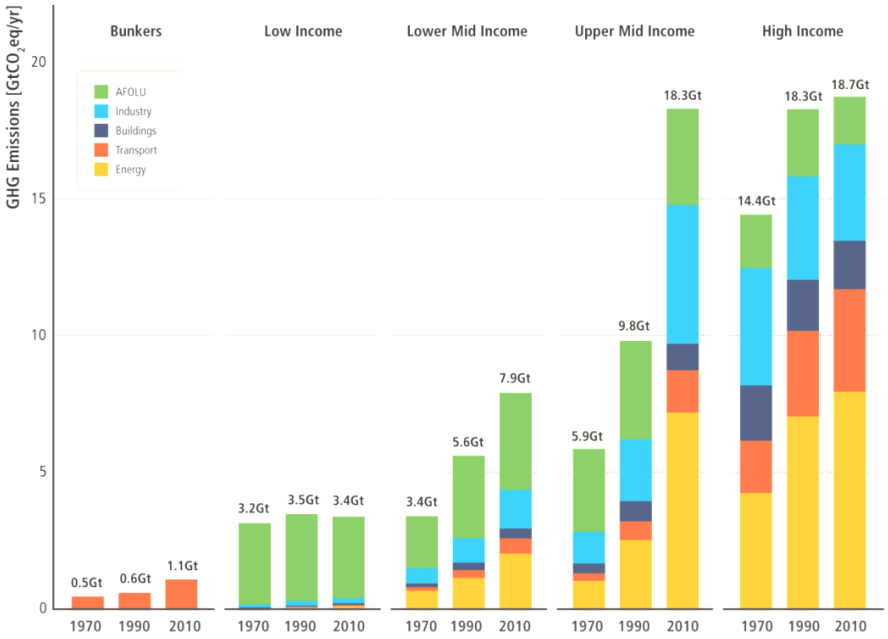

61. Measurements of CO2 in the atmosphere and in ice-trapped air show that GHGs have increased by about 40 per cent since 1800, with most of the increase occurring since the 1970s when global energy consumption accelerated (EEA, 2015a). Furthermore, measurements from ice cores suggest that current CO2 concentrations are higher than at any time in the last 800,000 years, with the 400 ppm milestone reached in 09/05/2013 (NOAA, 2015). Despite a growing number of climate mitigation measures, total global anthropogenic GHG emissions have grown continuously over the period 1970-2010, reaching their highest level in human history in 2000-2010 (Fig. 19); this trend continued in 2011-2016 (WMO, 2016).

62. In 2011-14, CO_2 and N_2O concentration had growth rates slightly higher than the 1995-2014 average. CH_4 concentration also showed growth, following a period of little change in 1999-2006 (WMO, 2016). During the 2014 and 2015, the annual mean concentrations of GHGs increased; in 2014, CO_2, CH_4 and N_2O concentrations were 397

ppm, 1833 ppb, and 327.1 ppb, respectively (NOAA, 2015). Approximately 44 per cent of the total CO_2 emitted by human activities from 2004 to 2013 may remain in the atmosphere, with the remaining 56 per cent stored in the oceans and the terrestrial biosphere (WMO, 2014, 2016).

63. Breakdown of the total anthropogenic GHG emissions in 2010 revealed that CO2 accounted for 76 per cent (65 per cent due to fossil fuel combustion/industry and 11per cent due to land-use), CH4 for 16 per cent, N2O for 6 per cent and fluorinated gases for 2per cent of the emissions (IPCC, 2014). Analysis of the total CO2 emissions from combustion for the period 1971-2010 showed that the primary drivers of the increasing trend are population growth and patterns of consumption/production (IPCC, 2014). Assessment of the CO2 emissions in relation to country income shows that these doubled for upper-mid-income countries (e.g. China and South Africa) for the period 1990-2010, almost reaching the level of high income countries (e.g. the US and most EU countries) (Fig. 20). A notable increase of CO2 emissions was also found in lower-mid-income countries (IPCC, 2014).